

## Simulated microgravity-cultured mesenchymal stem cells improve recovery following spinal cord ischemia in rats



Tomoyuki Kurose<sup>a</sup>, Shinya Takahashi<sup>b</sup>, Takashi Otsuka<sup>a</sup>, Kei Nakagawa<sup>a</sup>, Takeshi Imura<sup>a</sup>, Taijiro Sueda<sup>c</sup>, Louis Yuge<sup>a,\*</sup>

<sup>a</sup> Division of Bio-Environmental Adaptation Sciences, Graduate School of Biomedical and Health Sciences, Hiroshima University, Hiroshima, Japan

<sup>b</sup> Department of Cardiovascular Surgery, Hiroshima University Hospital, Hiroshima, Japan

<sup>c</sup> Hiroshima City Medical Association-administered Hiroshima City Aki Hospital, Hiroshima, Japan

### ARTICLE INFO

#### Keywords:

Microgravity  
Spinal cord  
Ischemia – reperfusion injury  
Motor function  
Astrocyte  
Brain-derived neurotrophic factor  
Apoptosis

### ABSTRACT

Spinal cord ischemia is a potential complication of thoracoabdominal aortic surgery that may induce irreversible motor disability. We investigated the therapeutic efficacy of simulated microgravity-cultured mesenchymal stem cell (MSC) injection following spinal cord ischemia – reperfusion injury. Sprague-Dawley rats were divided into sham, phosphate-buffered saline (PBS), normal gravity-cultured MSC (MSC-1 G), and simulated microgravity-cultured MSC (MSC-MG) groups. Spinal cord ischemia was induced by transient balloon occlusion of the thoracic aorta, which was followed immediately by PBS or MSC injection into the left carotid artery. Hindlimb motor function was evaluated by the Basso-Beattie-Bresnahan (BBB) scale. Spinal cords were removed 1, 3, or 7 days post-injury for immunohistochemical staining and Western blot analysis. One day post-injury, a few infiltrating inflammatory cells and small vacuoles were observed without significant group differences, followed over several days by progressive spinal cord degeneration. Glial fibrillary acidic protein (GFAP)-positive (reactive) astrocyte numbers were increased in all three groups, and brain-derived neurotrophic factor (BDNF) was co-localized with GFAP-positive cells in spinal ventral horn. Animals in the MSC-MG group demonstrated greater BDNF-positive astrocyte numbers, reduced caspase-3-positive cell numbers, and superior motor recovery. Microgravity-cultured MSC-based therapy may improve functional recovery following spinal ischemia – reperfusion injury by promoting astrocytic BDNF release, thereby preventing apoptosis.

### Abbreviations

BDNF	brain-derived neurotrophic factor
PBS	phosphate-buffered saline
MSC	mesenchymal stem cell
MG	microgravity
BBB	Basso-Beattie-Bresnahan
GFAP	glial fibrillary acidic protein
CNS	central nervous system
NT3	neurotrophin-3
BM	bone marrow
DMEM	Dulbecco's modified Eagle medium
FBS	fetal bovine serum
SCI	spinal cord injury

### 1. Introduction

Spinal cord ischemia and ensuing paraplegia are potentially devastating complications of thoracoabdominal aortic surgeries (Etz et al., 2008; Conrad et al., 2008), and there are currently no prophylactic or post-injury therapies that can substantially improve motor outcome following prolonged spinal ischemia – reperfusion injury. We recently demonstrated that mesenchymal stem cell (MSC) injection improves hindlimb function in a spinal injury model by preventing apoptosis of spinal cord neurons (Takahashi et al., 2018), suggesting that MSCs are a potentially valuable candidate for cell-based therapy. Indeed, MSCs prevent neural damage and improve function in experimental injury and disease models (Joyce et al., 2010) by promoting neuronal growth, reducing free radical generation and apoptosis, facilitating synaptic reconnection among damaged neurons, and by suppressing neuroinflammation. Furthermore, simulated microgravity-cultured MSCs were

\* Corresponding author: Bio-Environmental Adaptation Sciences, Graduate School of Biomedical and Health Sciences, Hiroshima University, 1-2-3 Kasumi, Minami-ku, Hiroshima 734-8551, Japan.

E-mail address: [ryuge@hiroshima-u.ac.jp](mailto:ryuge@hiroshima-u.ac.jp) (L. Yuge).

<https://doi.org/10.1016/j.scr.2019.101601>

Received 3 April 2019; Received in revised form 14 September 2019; Accepted 23 September 2019

Available online 15 October 2019

1873-5061/ © 2019 The Author(s). Published by Elsevier B.V. This is an open access article under the CC BY license (<http://creativecommons.org/licenses/by/4.0/>).

reported to be more effective than MSCs cultured under normal gravity (Yuge et al., 2006, 2011; Mitsuhashi et al., 2013).

Little is known of how MSCs act to prevent central nervous system damage or promote repair. Otsuka et al. (2018) reported that simulated microgravity-cultured MSCs promoted functional recovery in an animal model of brain damage and inhibited acute inflammation and apoptosis after injury both in vivo and in vitro. The cell culture environment is a critical factor influencing the therapeutic potential of MSCs after transplantation. However, the neuroprotective mechanisms of simulated microgravity-cultured MSCs have not been identified.

After neural damage, several cell types contribute to neural circuit repair. Astrocytes, the most numerous glial cell types, proliferate and show phenotypic transformation (activation) at the site of spinal cord injury. Various factors released from neighboring cells are reported to activate astrocytes. These reactive astrocytes are the main cellular component of the glial scar formed in response to injury (Hammond et al., 2014, 2015; Adams and Gallo, 2018). While these glial scars are traditionally thought to obstruct the central nervous system (CNS) regeneration, there is also evidence that glial scars can support CNS repair. Reactive astrocytes induced by ischemia appear to acquire a more protective phenotype by increasing expression of neurotrophic factors (Hayakawa et al., 2016; Zamanian et al., 2012), such as brain-derived neurotrophic factor (BDNF) and neurotrophin-3 (NT3), which enhance neuronal survival and axon regeneration (Dougherty et al., 2015). However, the contributions of glial cells and neurotrophic factors to the beneficial effects of MSCs following ischemic spinal cord injury are unclear.

In this study, we investigated the effects of MSCs after ischemic spinal cord injury on astrocyte phenotype, BDNF expression, and functional recovery. Moreover, we compared MSCs cultured under normal gravity to MSCs cultured in microgravity.

## 2. Material and methods

### 2.1. Animal care

All study protocols were approved by the Animal Testing Committee of Hiroshima University, and the Animal Testing Facility of the Hiroshima University Natural Science Support Center, Japan. Animal care and handling procedures were in accordance with National Institutes of Health guidelines.

### 2.2. Preparation of MSCs

Bone marrow (BM) cells were obtained from the bilateral femoral and tibial bones of 5-week-old male Sprague-Dawley rats under aseptic conditions. Isolated BM cells ( $1.0 \times 10^6$ ) were then suspended in low-glucose Dulbecco's modified Eagle medium (DMEM, Sigma-Aldrich Co, St. Louis, MO) supplemented with 10% fetal bovine serum (FBS, Thermo Fisher Scientific HyClone, South Logan, UT), penicillin (100 U/mL), and streptomycin (100 mg/mL; both from Sigma-Aldrich) in 90-mm diameter culture dishes (Sumitomo Bakelite Co, Tokyo, Japan). Cells were maintained in a 5% CO<sub>2</sub> humidified incubator at 37 °C, and the medium was exchanged after 48 h to eliminate floating cells. Cells adhering to the bottom of the culture dish were used to establish MSC cultures.

Adherent cells (MSCs) were seeded ( $3.5 \times 10^3$  cells/cm<sup>2</sup>) onto culture flasks and after 24 h of culture, randomly divided and subjected to continued culture in normal gravity (1 G) or simulated microgravity (MG). The MG condition was produced using Gravite® (Space-Bio-Laboratories Co. Ltd., Hiroshima, Japan). This device produces an environment similar to that of outer space ( $10^{-3}$  G) by rotating a sample around two axes, integrating the gravity vector with the temporal axis. The main unit size is 425 mm wide × 420 mm deep × 445 mm high. This is accomplished by rotation of a chamber at the center of the device, resulting in the uniform dispersion of the gravity vector within a

spherical volume, with a constant angular velocity. These specific conditions produced a simulated environment of  $10^{-3}$  G measured by gravity acceleration sensor, and it was defined as simulated microgravity.

### 2.3. Surgical procedures

Total 60 male Sprague-Dawley rats were housed and maintained on a 12-hour light/dark cycle with free access to food and water. Room temperature was maintained at 22 °C. Spinal cord injury (SCI) was induced using methods modified from Taira and colleagues and Saito and colleagues. General anesthesia was induced by placing the animals in a plastic chamber filled with 4.0% (vol/vol) isoflurane and then maintained by applying a face mask connected to a gaseous anesthesia system delivering 2.0% (vol/vol) isoflurane. Paravertebral temperature was monitored with a thermometer inserted into the paravertebral muscle and maintained at  $38.0 \pm 0.2$  °C with a heating pad. Rectal temperature was maintained below 36.5 °C to prevent visceral organ damage during spinal ischemic injury. SCI was induced by placement of a balloon-tipped catheter in the aorta. After heparin (200 U) administration, a 2-French Fogarty catheter (Fogarty Arterial Embolectomy Catheter; Edwards Lifesciences, Irvine, CA) was inserted through the left femoral artery into the descending thoracic aorta until the catheter tip reached the left subclavian artery (~12.5 cm from the site of insertion). The left carotid artery was exposed and ligated at the distal side and cannulated from the proximal side with a 20-gauge intravenous catheter, which was connected to an external blood reservoir positioned 54 cm above the body of the rat to control proximal aortic pressure at 40 mmHg. The tail artery pressure was measured with a noninvasive sphygmomanometer (BP-98A-L; Softron, Tokyo, Japan) as distal arterial blood pressure. Blood was allowed to flow into the external reservoir until the proximal blood pressure decreased to 40–45 mm Hg, which required approximately 90 s. The Fogarty catheter was then inflated with 0.05 mL saline. Aortic occlusion was confirmed by a sudden and complete loss of the distal arterial pressure. After 11 min of aortic occlusion, the balloon was deflated, and the blood in the reservoir was reinfused into the rat within 1 min. The 11-min balloon-occlusion time was determined from a series of preliminary experiments. Blood pressure was confirmed to increase by more than 80 mmHg following balloon deflation. The rats were divided into three groups immediately after reperfusion. In MSC-1 G and MSC-MG groups, MSCs were injected into the left carotid artery under balloon occlusion of the infrarenal aorta (5 cm from the insertion site), which prevented cells from flowing into the lower limb. In the PBS group, PBS was injected in the same manner under balloon occlusion of the infrarenal aorta. The fourth group received sham operation. In the sham group, all catheters, including the aortic balloon, were inserted in the same manner, but the balloon was not inflated. After removal of catheters and wound closure, the animals were returned to their home cages and allowed to recover.

### 2.4. Assessment of hindlimb motor function

Motor function was assessed postoperatively by an observer blinded to the treatment history of the individual animals. Hindlimb motor function was evaluated using the Basso-Beattie-Bresnahan (BBB) locomotor rating scale and inclined plane test. Briefly, the BBB scale evaluates hindlimb and joint movements, weight-bearing ability, forelimb–hindlimb coordination, paw position, and tail elevation, with scores ranging from 0 (no movement of the hindlimbs) to 21 (normal movement). The inclined plane test assesses the maximum angle at which the rat can maintain its position for 5 s.

### 2.5. Histology and immunohistochemistry

Nine rats from each group were euthanized, and 4%

paraformaldehyde was injected into the heart. Spinal cords were removed, incubated in 4% paraformaldehyde, and processed for paraffin embedding using standard methods. Before embedding, the spinal cord was minced at 5 mm intervals, and paraffin blocks were made with 12–13 divided spinal cords. Transverse sections were cut and stained with hematoxylin and eosin (HE) or prepared for immunohistochemistry.

For antibody labeling, paraffin sections were deparaffinized in xylene, rehydrated in a graded ethanol series, and incubated in methanol containing 0.3% H<sub>2</sub>O<sub>2</sub> for 20 min to quench endogenous peroxidases, followed by incubation in 1% normal horse serum or goat serum in PBS for 30 min to block non-specific binding. Sections were then incubated overnight at 4 °C with one of the following primary antibodies: anti-Tuj1 (GTX631836, Genetex Inc, Irvine, CA), anti-GFAP (#3670S, Cell Signaling Technology, Danvers, MA), or anti-caspase-3 (GTX110543, Genetex Inc). Sections were then treated with anti-rabbit or anti-mouse IgG conjugated to horseradish peroxidase (HRP)-polymer (ImmPress Reagent; Vector Laboratories, Burlingame, CA) for 60 min at room temperature. Immunolabeling was visualized by incubation with diaminobenzidine–hydrogen peroxide solution. Sections were then counterstained with hematoxylin. Tuj1 positive sites were considered as viable neurons, and Tuj1 positive areas were measured using ImageJ software. Tuj1 negative sites were considered as damaged neurons, and the areas were also measured.

## 2.6. Double immunostaining for BDNF and the astrocytic marker GFAP

Paraffin-embedded sections were rehydrated using xylene and graded ethanol solutions, and then heated to 98 °C for 15 min in antigen retrieval solution. After treatment with 1% normal goat serum in PBS for 30 min to block non-specific binding, the sections were treated with rabbit anti-BDNF antibody (sc-546, Santa Cruz Biotechnology, Santa Cruz, CA, USA) overnight at 4 °C, followed by FITC-labeled anti-rabbit IgG for 60 min at room temperature. Sections were treated with mouse anti-GFAP antibody overnight at 4 °C, then with Texas Red-labeled anti-mouse IgG for 60 min at room temperature. The sections were covered with Vectashield containing DAPI (H-1200, Vector) to stain cell nuclei.

## 2.7. Western blot analysis

Six rats from each group were euthanized and spinal cords removed, frozen, lysed in TRI Reagent (TR118, Molecular Research Center, Inc, USA), and centrifuged. The supernatants were stored at –80 °C until SDS-PAGE. Equal amounts of protein per lane were loaded on 8% polyacrylamide gels, separated by SDS-PAGE, and transferred to PDVF membranes. Membranes were blocked with 1% bovine serum albumin and immunolabeled with rabbit anti-BDNF antibody, followed by incubation with HRP-labeled anti-rabbit IgG antibody and SuperSignal West Pico Chemiluminescent Substrate (Thermo Fisher Scientific Inc, USA). Blots were then stripped with 50 mM glycine (pH 2.3) and re-probed with HRP-labeled anti-β-actin antibody (A2066, Sigma–Aldrich). The Western blotting results presented include representative images of the blots adjusted for contrast and densitometry of each band normalized to β-actin.

## 2.8. Reverse transcription and real-time polymerase chain reaction

When cultured cells reached confluency on dishes using DMEM-L growth medium, they were collected in PBS. Total RNA was extracted with NucleoSpin RNA (MACHERY- NAGEL GmbH & Co. KG, Düren, Germany). Reverse transcription was performed with ReverTra Ace-α (Toyobo Co., Ltd., Osaka, Japan). Using cDNA as the template, real-time polymerase chain reaction (PCR) was performed with the 7500 Real-time PCR system (Applied Biosystems, Carlsbad, CA). *Bdnf* was used as neurotrophic factors, and β-actin (*Actb*) was used as an internal endogenous control.

## 2.9. Statistical analysis

Hindlimb motor function scores were analyzed using two-way repeated-measures ANOVA followed by multiple group comparisons among time points. BDNF level from Western blot were compared by one-way ANOVA followed by Turkey–Kramer multiple comparison tests. *Bdnf* mRNA level were compared by unpaired *t*-test. All values are shown as mean ± standard deviations. *P* < 0.05 (two-tailed) was considered statistically significant for all tests.

## 3. Results

### 3.1. Locomotor dysfunction following ISC was improved by MSC treatment

After ischemia–reperfusion injury, most rats showed acute flaccid paraparesis and could not walk or sit on their hindlimbs. At 24 h post-injury, however, rats in the MSC-1 G and MSC-MG groups could sit up on their hindlimbs, while flaccid paraparesis continued in the PBS group. No signs of injury were apparent in the sham group. The BBB scores were numerically higher in the MSC-1 G group and significantly higher in the MSC-MG group compared to the PBS group at 24 h and day 3 post-SCI (Fig. 1A). Consistent with BBB results, the inclined plane test demonstrated greater performance (ability to maintain position at a higher angle) in the MSC-MG group at 24 h and day 3 post-SCI (Fig. 1B). Therefore, MSC treatment, particularly MSC-MG treatment, significantly accelerated recovery of locomotor function following SCI.

### 3.2. Microgravity-cultured MSCs promoted astrocytic BDNF expression

In the sham group, spinal structure was normal at both the gross and microstructural levels. No macroscopic changes were observed in spinal cords of the PBS, MSC-1 G, and MSC-MG groups at 1 day post-SCI, but microscopic observation revealed mild degeneration at the lumbar level (Fig. 2). Lumbar cross-sections of these spinal cords revealed a few infiltrating inflammatory cells in the gray matter and small vacuoles in white matter with no significant differences among groups. Degeneration of the spinal cord gradually worsened thereafter, particularly in the PBS group, with increased numbers of infiltrating cells and vacuoles appearing on days 3 and 7 post-SCI. Neurons and neuronal fibers were immunostained with Tuj1, but vacuoles in gray matter were Tuj1-negative (Fig. 3). Many such vacuoles were observed near the central canal, with fewer in the frontal and lateral areas of the ventral horn. These negatively stained areas were largest in the PBS group and smallest in the MSC-MG group. Therefore, MSC therapy, especially MSC-MG therapy, reduced neurodegeneration and reduced inflammatory cell infiltration.

Increased numbers of GFAP-positive cells were observed in gray matter following SCI (Fig. 4). These cells exhibited elongated processes compared to GFAP-positive cells of the sham group. Astrocytes in the PBS group spinal cord exhibited the most elongated processes, and these cells were concentrated around border areas between gray and white matter. Astrocytes had shorter processes in MSC-1 G and MSC-MG groups compared to the PBS group. In addition, astrocytes were more scattered in ventral horn of the MSC-MG group.

Immunoexpression of BDNF was colocalized with GFAP, especially in the ventral horn (Fig. 5). These BDNF-positive astrocytes were more numerous in the MSC-MG group than the other groups. Western blot analysis was applied to quantify the level of BDNF expression. No signal or a very little signal was measured in the sham group (Fig. 6A). In accordance with previous studies, mature BDNF (mBDNF) and proBDNF expression levels were higher in the MSC-MG group than the PBS and MSC-1 G groups.

Neurotrophic factor gene expression in MSCs was analyzed using real-time PCR. The expression of BDNF in MSC-MG did not significantly increase than that in MSC-1 G (Fig. 6B).

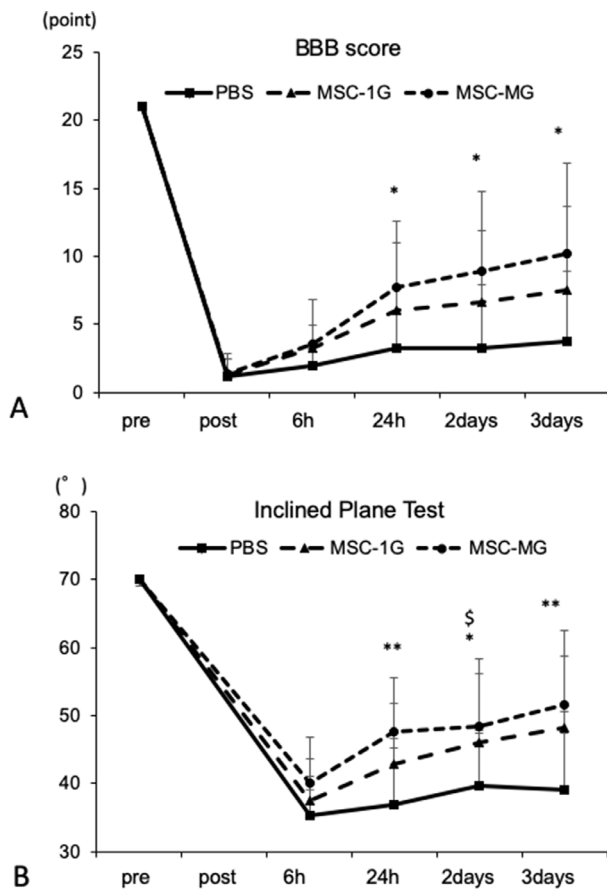


**Fig. 1.** Time-dependent changes in locomotor function following spinal ischemia-reperfusion injury in rats receiving PBS, mesenchymal stem cells (MSCs) cultured in normal gravity (MSC-1 G), or MSCs cultured in microgravity (MSC-MG). (A) Neurologic function was assessed using the BBB scale, which demonstrated faster and greater recovery in the MSC-MG group. The y-axis means the scale (0–21) represented sequential recovery stages and categorizes combinations of rat joint movement, hindlimb movements, stepping, forelimb and hindlimb coordination, trunk position and stability, paw placement and tail position. (B) Inclination angle at the moment of rat slippage is recorded. The maximum inclined plane angle was also larger in the MSC-MG group. In the graph, pre means before operation and post means immediately after operation. \*:  $p < 0.05$  PBS vs. MSC-MG, \*\*:  $p < 0.01$  PBS vs. MSC-MG, \$:  $p < 0.05$  PBS vs. MSC-1 G.

### 3.3. Microgravity-cultured MSCs prevented apoptosis following SCI

Immunoeexpression of the apoptosis marker caspase-3 was elevated in the spinal cord white matter nuclei of all experimental groups compared to the sham group (Fig. 7), but the number of caspase-3-positive cells in ventral horn was higher in the PBS group than the MSC-1 G and MSC-MG groups.

## 4. Discussion

The hind limbs of rats were paralyzed by a single ischemia. However, after the injection of MSCs, there was significant improvement in the hindlimb locomotor function. The hindlimb functions in MSC-MG group were more effective than those in MSC-1 G group. Therefore, treatment with MSC-MG is a potentially effective strategy for improving functional recovery following ischemic SCI.

To understand the effects of MSC-1 G and MSC-MG, we histologically examined the spinal cord. Histological observation revealed little gross structural alteration following SCI in any group, but immunohistochemical staining revealed group difference in astrocyte activation, local neurodegeneration, and BDNF expression among PBS, MSC-1 G, and MSC-MG groups. Inflammatory cell infiltration and vacuolization were more extensive in the PBS group than the MSC groups and lower in the MSC-MG group than the MSC-1 G group. Thus, the neuroprotective effect of microgravity-cultured MSC may be superior to other MSCs. Reactive astrocytes increased after ischemia-reperfusion injury, and these cells exhibited elongated processes, a phenotype that appears to hamper CNS repair. Astrocytes in injured CNS are activated by numerous factors released from neighboring microglia or leukocytes. Proliferating reactive astrocytes form glial scars that prevent neural growth and circuit reformation. However, a large number of studies have found that reactive astrocytes can also protect CNS cells and tissue (Faulkner et al., 2004; Myer et al., 2006).

MSCs secrete a number of neurotrophic and angiogenic factors that promote neuronal growth and differentiation, induce angiogenesis, neurogenesis and glial activation, and decrease apoptosis and inflammation (Castillo-Melendez et al., 2013). Real-time PCR revealed BDNF did not increase in MSC-1 G and MSC-MG, and thus the increment in BDNF was considered as that produced by cells in the host animal, and not by MSCs. MSC-secreted factors, such as TNF- $\alpha$  and IL-6, trigger neuroinflammation (Horn et al., 2011), and several inflammatory cytokines possibly activate astrocytes (Kuray et al., 2016). Simulated microgravity has been reported that altered the expression of trophic factors (Otsuka et al., 2018; Ratushnyy et al., 2018). In our experiments, the expression of trophic factors may have changed the

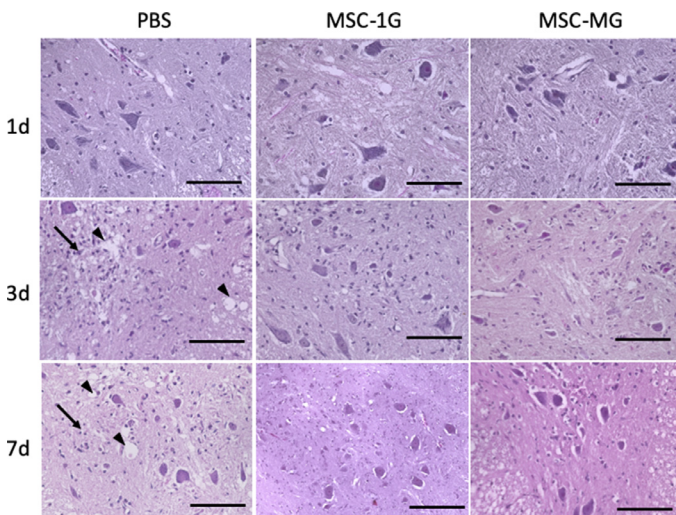


**Fig. 2.** Spinal cord injury as revealed by HE staining 1, 3, and 7 days following ischemia-reperfusion injury. The upper photograph is the spinal ventral horn 1 day after ischemia, the middle one is after 3 days, and the lower is after 7 days. The left column is the PBS group, the middle column is the 1 G group, and the right column is the microscopic image of the MG group. Vacuolization (arrow-head) of gray matter expanded post-injury in all groups but was greater in the PBS group than the MSC groups at 3 and 7 days. Infiltrating cells (arrow) were observed near vacuolized area. Bar = 100  $\mu$ m.

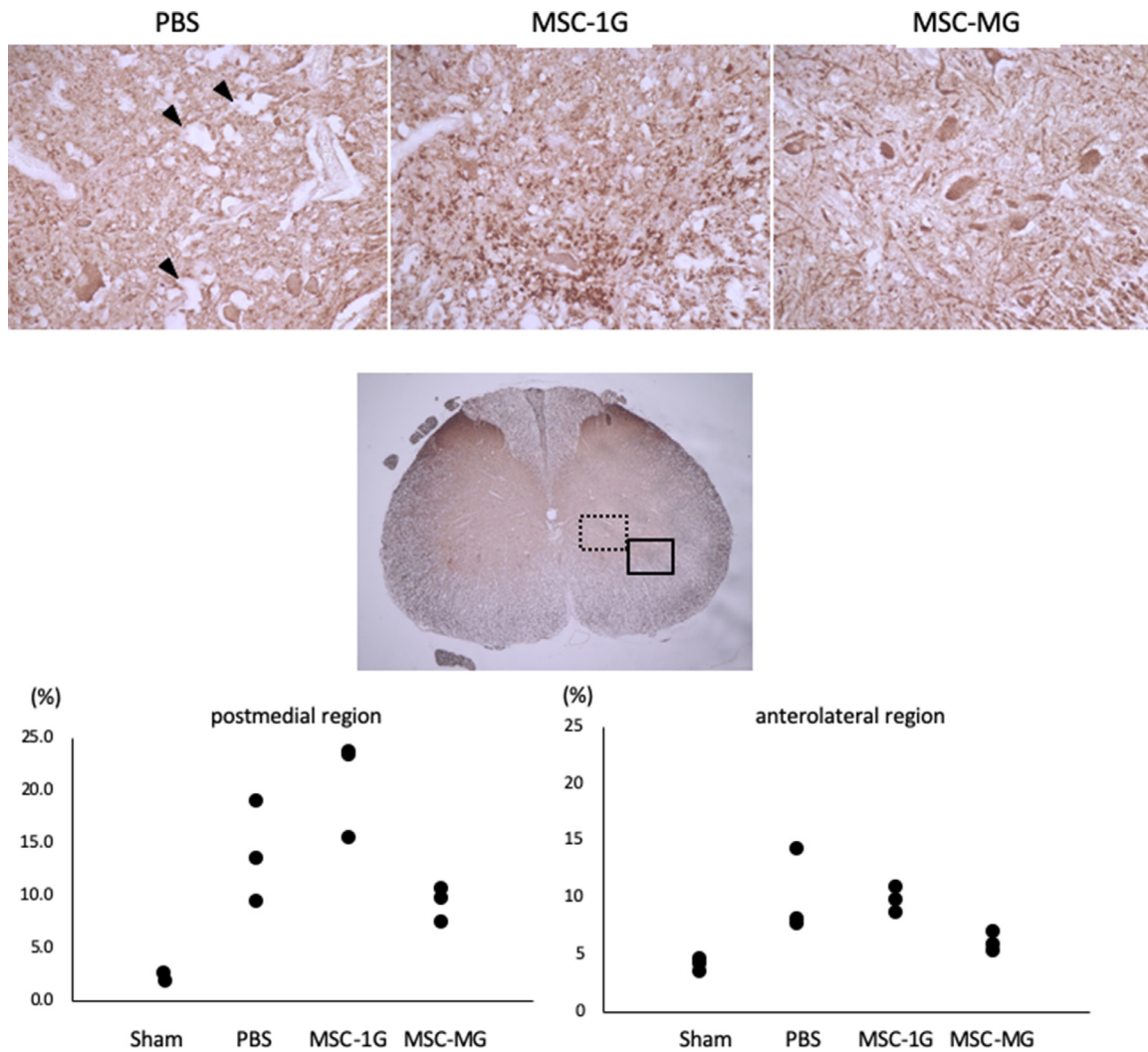


**Fig. 3.** Microscopic observation of Tuj1-positive cells and fibers in the spinal ventral horn. (A) Neural cells and neural fibers were strongly stained while vacuoles (arrowheads) in the gray matter were Tuj1-negative. The number of vacuoles was higher in the PBS group than the MSC groups. (B) The damaged area of the anterolateral region (square) and the postmedial region (dotted square) is shown in the graph. The damaged area of MSC-MG was smaller than that of the PBS and MSC-1 G. The damaged area (%) was measured by dividing the Tuj1 negative area by the gray matter area.

action on glial cells.

Although changes in BDNF were observed in the micrographs, quantification was difficult. The number of cells (DAPI stained) varied (23~116 / field of view), and the astrocyte projections were stained in small dots; astrocytes could not be counted accurately (15~136 / field of view). As a result, the proportion of BDNF positive astrocytes also

varied widely, and it was not possible to create accurate quantification rules. Since it was difficult to determine the amount of BDNF from the microscopic image, we measured the amount of BDNF by Western blot. The change in the expression level of BDNF by micrographs is considered to be supported by Western blot. Several studies have found enhanced expression of BDNF and neurotrophin-3 (NT3) in injured

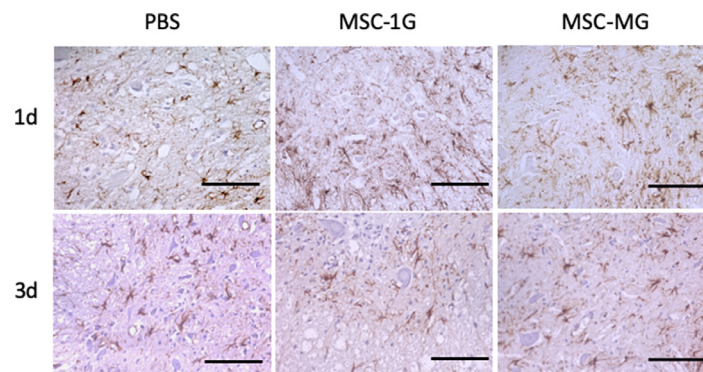


**Fig. 4.** Astrocyte activation in the ventral horn following ischemia-reperfusion injury. The reactive astrocytes with elongated processes increased in all groups following ischemia but were most numerous in the PBS group. Bar = 100  $\mu$ m.

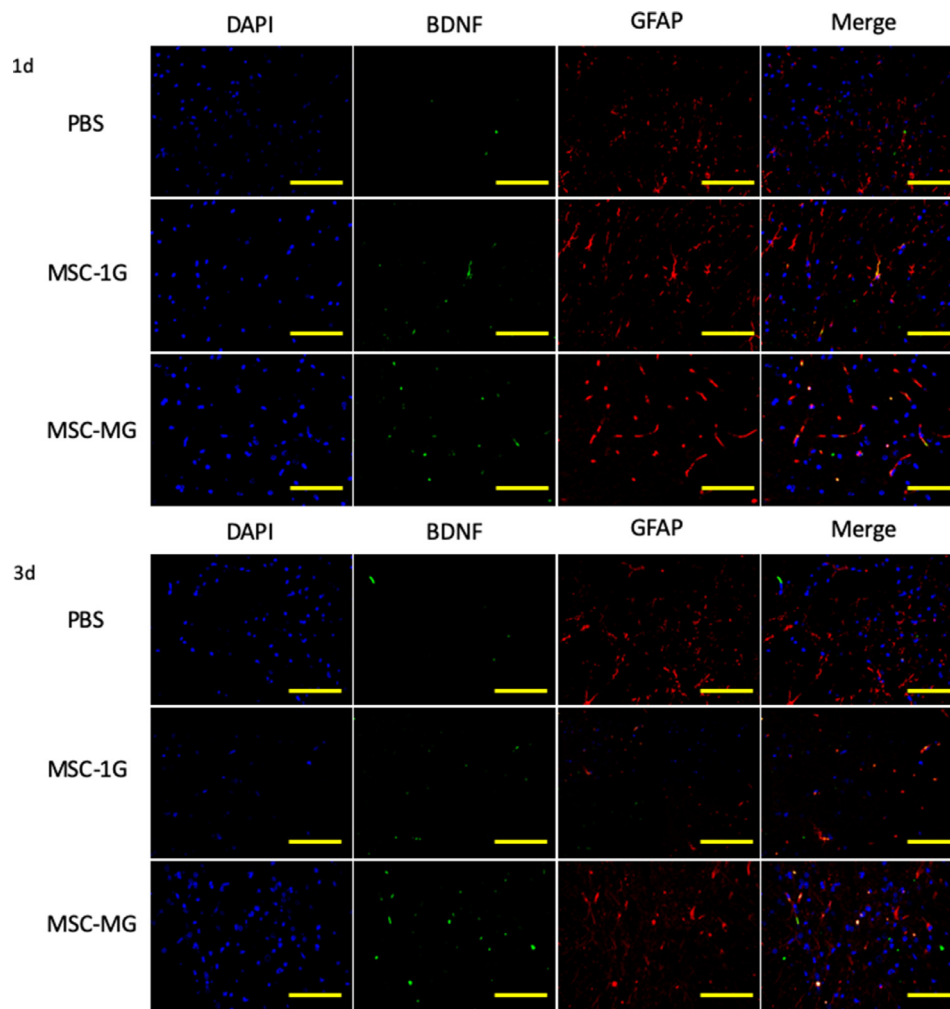


**Fig. 5.** Enhanced BDNF expression by astrocytes in spinal ventral horn following ischemia – reperfusion injury. Fluorescence images showed high BDNF expression (green) and colocalization of BDNF and GFAP (red). In the right column, BDNF-expressing astrocytes (yellow) in MSC-1G and MSC-MG are observed. Blue: DAPI. Bar = 50  $\mu$ m. (For interpretation of the references to color in this figure legend, the reader is referred to the web version of this article.)

spinal cord, trophic factors that can enhance neuron survival and axon regeneration (Dougherty et al., 2015; Mantilla et al., 2013; Batista et al., 2014; Gransee et al., 2015; Liu et al., 2017). BDNF is a ubiquitous neurotrophic factor produced by many neural cell types with well demonstrated capacity to promote neuronal growth and improve neural function (Joseph et al., 2012; Yang et al., 2017). Both immunohistochemistry and immunoblotting demonstrated higher BDNF expression in the MSC-MG group. Recently, several studies have reported anti-apoptotic effects of BDNF (Deng et al., 2015; Kim and Zhao, 2005). Kim and Zhao (2005) found that BDNF treatment inhibited caspase-3 activation following neuronal injury. These results are consistent with our findings that the greater increase in BDNF-positive astrocyte number was associated with lower caspase-3 immunorexpression following ischemia – reperfusion injury. Caspase-3 is an apoptosis effector located downstream of the apoptotic pathway, and a decrease in caspase-3 levels indicates suppression of apoptosis. Otsuka et al. (2018) reported that MSCs cultured under simulated microgravity facilitated functional recovery in a traumatic brain injury model through inhibition of inflammation and apoptosis. We suggest that these microgravity-cultured MSCs may have greater anti-apoptotic efficacy by promoting higher BDNF production in astrocytes, thereby rescuing neural cells in injured spinal cord and improving functional recovery.

Numerous studies have examined various cell-based therapies for improving recovery following SCI, but results are still unsatisfactory.

Simulated microgravity-cultured MSCs improved locomotor function in an SCI model, likely by reducing apoptosis through enhanced neurotrophic factor release from astrocytes at the injury site. In conclusion, our results suggest that injection of MSCs cultured under simulated microgravity is a potentially valuable strategy for cell-based treatment of SCI.

#### Disclosure statement

Conflicts of interest associated with this research have been approved by the Institutional Conflict of Interest Management Committee. By regularly reporting research progresses to the Conflicts of Interest Management Committee, we will maintain fairness regarding the reporting of this research.

#### Declaration of Competing Interest

This manuscript has not been published and is not under consideration for publication elsewhere. All the authors have read the manuscript and have approved this submission. The authors report no conflicts of interest. Every author listed meets the qualifications for authorship.

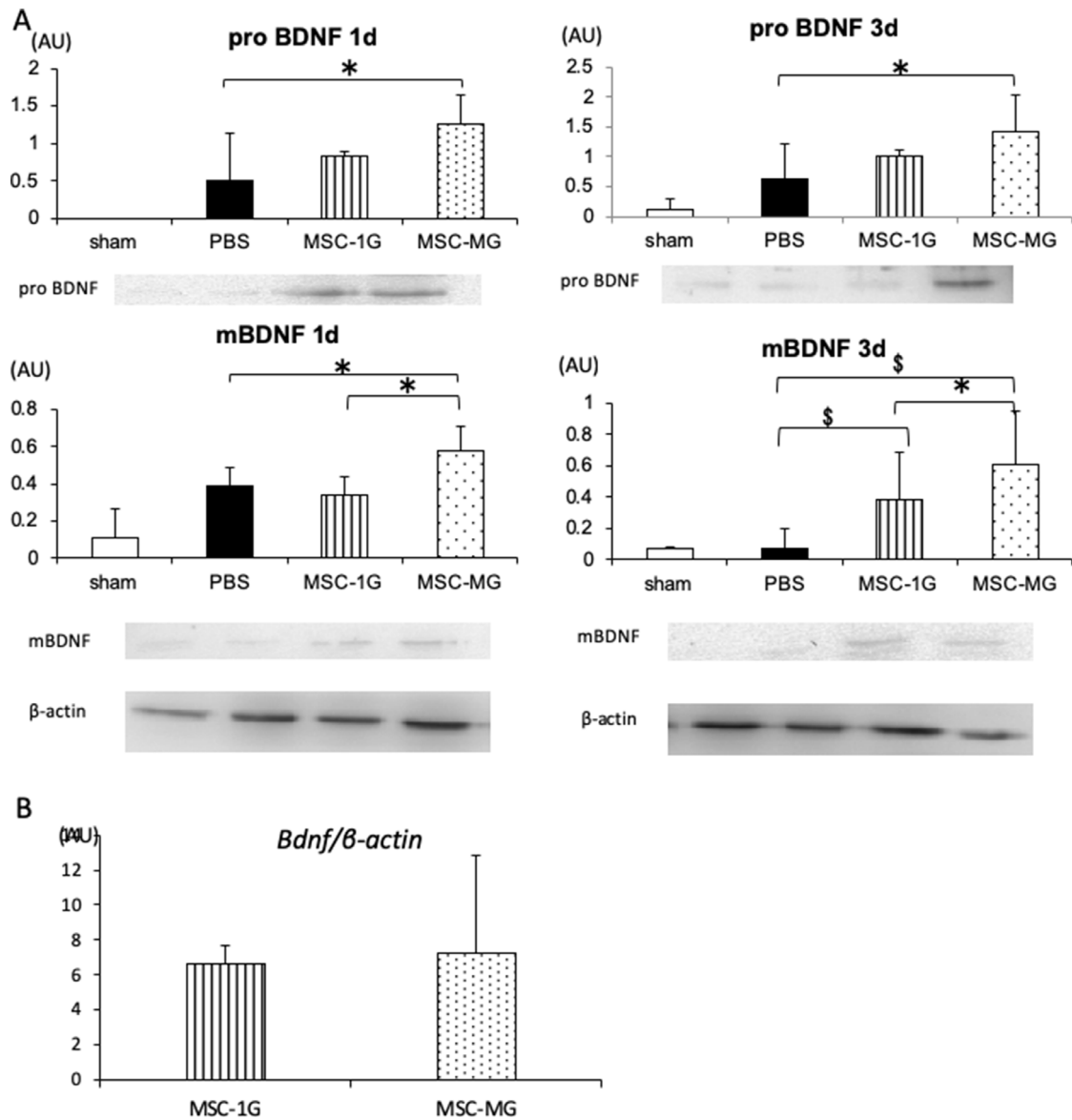


Fig. 6. (A) Bar graph showing pro-BDNF and mBDNF expression levels following ischemia – reperfusion injury. BDNF expression was highest in the MSC-MG group at 1 and 3 days after ischemia. (B) Bar graph showing Bdnf mRNA expression of MSCs cultured in normal gravity and simulated microgravity. No significant difference was observed in the two groups. \*:  $p < 0.05$ , \$:  $p < 0.01$ .

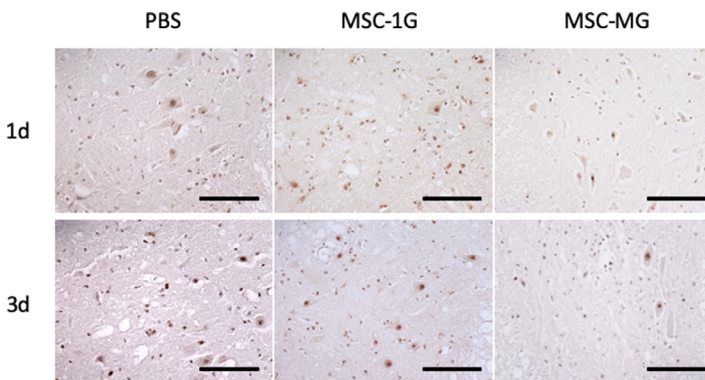


Fig. 7. Caspase-3 staining following ischemia – reperfusion injury showing reduced apoptosis in the MSC-MG group. Brown colored nuclei indicate the apoptotic cells, and blue nuclei indicate living cells. Scale bar = 100  $\mu$ m. (For interpretation of the references to color in this figure legend, the reader is referred to the web version of this article.)

Supplementary materials

Supplementary material associated with this article can be found, in the online version, at doi:10.1016/j.scr.2019.101601.

References

Adams, K.L., Gallo, V., 2018. The diversity and disparity of the glial scar. *Nat. Neurosci.* 21, 9–15.  
 Batista, C.M., Bianqui, L.L., Zanon, B.B., Ivo, M.M., Oliveira, G.P., Maximino, J.R., Chadi,

- G., 2014. Behavioral improvement and regulation of molecules related to neuroplasticity in ischemic rat spinal cord treated with PEDF. *Neural Plast.* 2014, 451639.
- Castillo-Melendez, M., Yawno, T., Jenkin, G., Miller, S.L., 2013. Stem cell therapy to protect and repair the developing brain: a review of mechanisms of action of cord blood and amnion epithelial derived cells. *Front. Neurosci.* 7, 194.
- Conrad, M.F., Ye, J.Y., Chung, T.K., Davison, J.K., Cambria, R.P., 2008. Spinal cord complications after thoracic aortic surgery: long-term survival and functional status varies with deficit severity. *J. Vasc. Surg.* 48, 47–53.
- Deng, H., Zuo, X., Zhang, J., Liu, X., Liu, L., Xu, Q., Wu, Z., Ji, A., 2015. A-lipoic acid protects against cerebral ischemia/reperfusion-induced injury in rats. *Mol. Med. Rep.* 11, 3659–3665.
- Etz, C.D., Luehr, M., Kari, F.A., Bodian, C.A., Smego, D., Plestis, K.A., Griep, R.B., 2008. Paraplegia after extensive thoracic and thoracoabdominal aortic aneurysm repair: does critical spinal cord ischemia occur postoperatively? *J. Thorac. Cardiovasc. Surg.* 135, 324–330.
- Faulkner, J.R., Herrmann, J.E., Woo, M.J., Tansey, K.E., Doan, N.B., Sofroniew, M.V., 2004. Reactive astrocytes protect tissue and preserve function after spinal cord injury. *J. Neurosci.* 24, 2143–2155.
- Gransee, H.M., Zhan, W.Z., Sieck, G.C., Mantilla, C.B., 2015. Localized delivery of brain-derived neurotrophic factor-expressing mesenchymal stem cells enhances functional recovery following cervical spinal cord injury. *J. Neurotrauma.* 32, 185–193.
- Hammond, T.R., McEllin, B., Morton, P.D., Raymond, M., Dupree, J., Gallo, V., 2015. Endothelin-B receptor activation in astrocytes regulates the rate of oligodendrocyte regeneration during remyelination. *Cell Rep.* 13, 2090–2097.
- Hammond, T.R., Gadea, A., Dupree, J., Kerninon, C., Nait-Oumesmar, B., Aguirre, A., Gallo, V., 2014. Astrocyte-derived endothelin-1 inhibits remyelination through notch activation. *Neuron* 81, 588–602.
- Hayakawa, K., Esposito, E., Wang, X., Terasaki, Y., Liu, Y., Xing, C., Ji, X., Lo, E.H., 2016. Transfer of mitochondria from astrocytes to neurons after stroke. *Nature* 535, 551–555.
- Horn, A.P., Bernardi, A., Luiz, Frozza, R., Grudzinski, P.B., Hoppe, J.B., de Souza, L.F., Chagastelles, P., de Souza, Wyse, A.T., Bernard, E.A., Battastini, A.M., Campos, M.M., Lenz, G., Nardi, N.B., Salbego, C., 2011. Mesenchymal stem cell-conditioned medium triggers neuroinflammation and reactive species generation in organotypic cultures of rat hippocampus. *Stem. Cells Dev.* 20, 1171–1181.
- Joseph, M.S., Tillakaratne, N.J., de Leon, R.D., 2012. Treadmill training stimulates brain-derived neurotrophic factor mRNA expression in motor neurons of the lumbar spinal cord in spinally transected rats. *Neuroscience* 224, 135–144.
- Joyce, N., Annett, G., Wirthlin, L., Olson, S., Bauer, G., Nolte, J.A., 2010. Mesenchymal stem cells for the treatment of neurodegenerative disease. *Regen. Med.* 5, 933–946.
- Kim, D.H., Zhao, X., 2005. BDNF protects neurons following injury by modulation of caspase activity. *Neurocrit. Care* 3, 71–76.
- Kiray, H., Lindsay, S.L., Hosseinzadeh, S., Barnett, S.C., 2016. The multifaceted role of astrocytes in regulating myelination. *Exp. Neurol.* 283 (Pt B), 541–549.
- Liu, Y., Yan, Y., Inagaki, Y., Logan, S., Bosnjak, Z.J., Bai, X., 2017. Insufficient astrocyte-derived brain-derived neurotrophic factor contributes to propofol-induced neuron death through Akt/glycogen synthase kinase 3 $\beta$ /mitochondrial fission pathway. *Anesth. Analg.* 125, 241–254.
- Mantilla, C.B., Gransee, H.M., Zhan, W.Z., Sieck, G.C., 2013. Motoneuron BDNF/TrkB signaling enhances functional recovery after cervical spinal cord injury. *exp. Neurol.* 247, 101–109.
- Mitsuhara, T., Takeda, M., Yamaguchi, S., Manabe, T., Matsumoto, M., Kawahara, Y., Yuge, L., Kurisu, K., 2013. Simulated microgravity facilitates cell migration and neuroprotection after bone marrow stromal cell transplantation in spinal cord injury. *Stem Cell Res. Ther.* 4, 35.
- Myer, D.J., Gurkoff, G.G., Lee, S.M., Hovda, D.A., Sofroniew, M.V., 2006. Essential protective roles of reactive astrocytes in traumatic brain injury. *Brain* 129, 2761–2772.
- Otsuka, T., Imura, T., Nakagawa, K., Shrestha, L., Takahashi, S., Kawahara, Y., Sueda, T., Kurisu, K., Yuge, L., 2018. Simulated microgravity culture enhances the neuroprotective effects of human cranial bone-derived mesenchymal stem cells in traumatic brain injury. *Stem. Cells Dev.* 27, 1287–1297.
- Ratushnyy, A., Ezdakova, M., Yakubets, D., Buravkova, L., 2018. angiogenic activity of human adipose-derived mesenchymal stem cells under simulated microgravity. *Stem Cells Dev.* 27, 831–837.
- Takahashi, S., Nakagawa, K., Tomiyasu, M., Nakashima, A., Katayama, K., Imura, T., Herlambang, B., Okubo, T., Arihiro, K., Kawahara, Y., Yuge, L., Sueda, T., 2018. Mesenchymal stem cell-based therapy improves lower limb movement after spinal cord ischemia in rats. *Ann. Thorac. Surg.* 105, 1523–1530.
- Yang, B., Qin, J., Nie, Y., Li, Y., Chen, Q., 2017. Brain-derived neurotrophic factor propeptide inhibits proliferation and induces apoptosis in C6 glioma cells. *Neuroreport* 28, 726–730.
- Yuge, L., Kajiume, T., Tahara, H., Kawahara, Y., Umeda, C., Yoshimoto, R., Wu, S.L., Yamaoka, K., Asashima, M., Kataoka, K., Ide, T., 2006. Microgravity potentiates stem cell proliferation while sustaining the capability of differentiation. *Stem Cells Dev.* 15, 921–929.
- Yuge, L., Sasaki, A., Kawahara, Y., Wu, S.L., Matsumoto, M., Manabe, T., Kajiume, T., Takeda, M., Magaki, T., Takahashi, T., Kurisu, K., Matsumoto, M., 2011. Simulated microgravity maintains the undifferentiated state and enhances the neural repair potential of bone marrow stromal cells. *Stem Cells Dev.* 20, 893–900.
- Zamanian, J.L., Xu, L., Foo, L.C., Nouri, N., Zhou, L., Giffard, R.G., Barres, B.A., 2012. Genomic analysis of reactive astroglia. *J. Neurosci.* 32, 6391–6410.